BEILSTEIN JOURNAL OF ORGANIC CHEMISTRY

Supporting Information

for

A *m*-quaterphenyl probe for absolute configurational assignments of primary and secondary amines

Yuka Takeuchi, Mutsumi Kobayashi, Yuuka Gotoh, Mari Ikeda, Yoichi Habata, Tomohiko Shirai and Shunsuke Kuwahara

Beilstein J. Org. Chem. **2025,** *21,* 2211–2219. doi:10.3762/bjoc.21.168

Experimental procedures, characterization data including copies of NMR spectra (^{1}H NMR, ^{13}C NMR), CD spectra of (*S*)-2f and (*R*)-2f, theoretical calculations, and X-ray structure of (*S*)-2b

Table of contents

Synthesis of conjugates (*S*)-2b–g, (*R*)-2f, and (*R*)-2h

(*S*)-2-[2,10-Bis(4-methoxyphenyl)-5,7-dihydro-6*H*-dibenzo[*c,e*]azepin-6-yl]-3-methylbutan-1-ol ((*S*)-2b)

Following general procedure was carried out with **1** (70.3 mg, 0.127 mmol), L-valinol (26.1 mg, 0.253 mmol) and K_2CO_3 (118 mg, 0.850 mmol) in CH_3CN (4 mL) at 85 °C for 4 h. Purification using column chromatography (hexane/EtOAc, v/v 1:1) afforded amine (*S*)-**2b** (59.6 mg, 95% yield) as colorless prisms: mp 148.1–149.1 °C; ^{1}H NMR (400 MHz, $CDCl_3$) δ 7.74 (d, J = 1.8 Hz, 2H), 7.61–7.56 (m, 6H), 7.41 (d, J = 7.8 Hz, 2H), 6.99 (dt, J_1 = 8.7 Hz, J_2 = 3.8 Hz, 4H), 3.85 (s, 6H), 3.75–3.68 (m, 5H), 3.48 (t, J = 9.4 Hz, 4H), 2.67 (ddd, J_1 = 9.4 Hz, J_2 = 5.1 Hz, J_3 = 3.8 Hz, 1H), 2.01 (sep.d, J_1 = 6.9 Hz, J_2 = 5.1 Hz, 1H), 0.93 (dd, J_1 = 6.9 Hz, J_2 = 3.1 Hz, 6H); ^{13}C NMR (100 MHz, $CDCl_3$) δ 159.3, 141.3, 140.6, 134.2, 133.2, 130.1, 128.2, 126.4, 126.1, 114.3, 71.9, 59.8, 55.4, 52.1. 29.0, 23.0, 19.5; IR (KBr) ν_{max} = 3385, 2952, 2834, 1607, 1518, 1489, 1462, 1247, 1180, 1037, 1013, 820 cm^{-1}; FAB-MS (matrix DTT/TG = 1:1) *m/z* 494 $[M]^+$ 100%; Anal. Calcd for $C_{33}H_{35}NO_3$: C, 80.29; H, 7.15; N, 2.84. Found. C, 80.03; H, 7.09; N, 2.86.

(*S*)-2-[2,10-Bis(4-methoxyphenyl)-5,7-dihydro-6*H*-dibenzo[*c,e*]azepin-6-yl]-2-phenylethanol ((*S*)-2c)

Following general procedure was carried out with **1** (71.9 mg, 0.130 mmol), (*S*)-2-phenylglycinol (24.0 mg, 0.175 mmol) and K_2CO_3 (98.7 mg, 0.714 mmol) in CH_3CN (4 mL) at 85 °C for 3 h. Purification using column chromatography (hexane/EtOAc, v/v 2:1) afforded amine (*S*)-**2c** (58.9 mg, 87% yield) as colorless solid: mp 178.0–179.5 °C; ^{1}H NMR (400 MHz, $CDCl_3$) δ 7.72 (d, J = 1.8 Hz, 2H), 7.58 (dt, J_1 = 8.8 Hz, J_2 = 4.0 Hz, 4H), 7.53–7.32 (m, 7H), 7.26–7.25 (m, 2H), 6.99 (dt, J_1 = 8.8 Hz, J_2 = 4.0 Hz, 4H), 4.03 (dd, J_1 = 11.1 Hz, J_2 = 4.8 Hz, 1H), 3.93 (dd, J_1 = 11.1 Hz, J_2 = 4.8 Hz, 1H), 3.85 (s, 6H), 3.76 (t, J = 4.8 Hz, 1H), 3.66 (d, J = 12.4 Hz, 1H), 3.47 (d, J = 12.4 Hz, 1H), 2.27 (br, 1H); ^{13}C NMR (100 MHz, $CDCl_3$) δ 159.3, 141.6, 140.7, 133.3, 133.2, 130.3, 128.8, 128.7, 128.2, 127.9, 126.0, 125.8, 114.3, 68.5, 64.0, 55.4, 52.6; IR (KBr) ν_{max} = 3417, 3025, 2931, 2834, 1608, 1517, 1489. 1454, 1248, 1178, 1029, 820 cm^{-1}; FAB-MS (matrix DTT/TG = 1:1) *m/z* 529 $[M+1]^+$ 100%; Anal. Calcd for $C_{36}H_{33}NO_3$: C, 81.95; H, 6.30; N, 2.65. Found. C, 81.70; H, 6.33; N, 2.60.

Methyl (*S*)-2-(2,10-bis(4-methoxyphenyl)-5,7-dihydro-6*H*-dibenzo[*c,e*]azepin-6-yl)propanoate ((*S*)-2d)

Following general procedure was carried out with **1** (100.0 mg, 0.182 mmol), L-alanine methyl ester hydrochloride (28.3 mg, 0.203 mmol) and K_2CO_3 (150.0 mg, 1.09 mmol) in CH_3CN (6 mL) at 60 °C for 19 h. Purification using column chromatography (hexane/EtOAc, v/v 1:1) afforded amine (*S*)-**2d** (71.4 mg, 80% yield) as colorless solid: mp 62.9 °C (dec.); ^{1}H NMR (400 MHz, $CDCl_3$) δ 7.73 (d, J = 1.8 Hz, 2H), 7.62–7.55 (m, 6H), 7.43 (d, J = 7.9 Hz, 2H), 7.00 (dt, J_1 = 8.8 Hz, J_2 = 3.0 Hz, 4H), 3.86 (s, 6H), 3.74 (s, 3H), 3.68–3.54 (m, 5H), 1.50 (d, J = 6.9 Hz); ^{13}C NMR (100 MHz, $CDCl_3$) δ 174.4, 159.3, 141.5, 140.7, 133.3, 132.8, 130.6, 128.2, 126.0, 125.9, 114.3, 61.6, 55.4, 52.6, 51.9, 16.8; IR (KBr) ν_{max} = 3024, 2950, 1730, 1608, 1517, 1489, 1248, 1178, 1029, 821 cm^{-1}; FAB-MS (matrix: DTT:TG = 1:1) *m/z* 493($[M]^+$ 55%), Anal. Calcd. for $C_{32}H_{31}NO_4 \cdot 0.3H_2O$: C, 77.02; H, 6.38; N, 2.81. Found: C, 76.93; H, 6.09; N, 2.82.

Methyl (*S*)-2-(2,10-bis(4-methoxyphenyl)-5,7-dihydro-6*H*-dibenzo[*c,e*]azepin-6-yl)-3-hydroxypropanoate ((*S*)-2e)

Following general procedure was carried out with **1** (101.0 mg, 0.182 mmol), L-serine methyl ester hydrochloride (32.1 mg, 0.206 mmol) and K_2CO_3 (150.0 mg, 1.09 mmol) in CH_3CN (6 mL) at 50 °C for 18 h. Purification using column chromatography (EtOAc) afforded amine (*S*)-**2e** (76.3 mg, 82% yield) as colorless solid: mp 110.0 °C (dec.); ^{1}H NMR (400 MHz, $CDCl_3$) δ 7.72 (d, J = 1.8 Hz, 2H), 7.61–7.56 (m, 6H), 7.39 (d, J = 7.8 Hz, 2H), 7.00 (dt, J_1 = 8.7 Hz, J_2 = 3.1 Hz, 4H), 3.97–3.88 (m, 2H), 3.86 (s, 6H), 3.69 (s, 4H), 3.62–3.59 (dd, J_1 = 5.9 Hz, J_2 = 5.9 Hz, 1H), 3.56 (s, 3H); ^{13}C NMR (100 MHz, $CDCl_3$) δ 172.2, 159.3, 141.3, 140.8, 133.2, 132.9, 130.5, 128.2, 126.1, 126.0, 114.3, 66.5, 59.5, 55.4, 52.3, 51.5; IR (KBr) ν_{max} = 3423, 3025, 2951, 1730, 1608, 15178, 1490, 1248, 1178, 1038, 821 cm^{-1}; FAB-MS (matrix: *m*-NBA) *m/z* 509 ([M]$^+$ 68%), Anal. Calcd. for $C_{32}H_{31}NO_5 \cdot 0.12CHCl_3$: C, 73.63; H, 5.99; N, 2.67. Found: C, 73.49; H, 5.80; N, 2.66.

(*S*)-2,10-Bis(4-methoxyphenyl)-6-(1-phenylethyl)-6-propyl-6,7-dihydro-5*H*-dibenzo[*c,e*]azepin-6-ium bromide ((*S*)-2f)

Following general procedure was carried out with **1** (70.0 mg, 0.127 mmol), (*S*)-*N*-(1-phenylethyl)propan-1-amine [1] (23.1 mg, 0.142 mmol) and K_2CO_3 (110 mg, 0.799 mmol) in CH_3CN (4 mL) at 85 °C for 23 h. Purification using column chromatography ($CHCl_3$/MeOH, v/v 5:1) afforded ammonium salt (*S*)-**2f** (50.0 mg, 62% yield) as pale yellow solid: m.p. 125.1–126.1 °C; ^{1}H NMR (400 MHz, $CDCl_3$) δ 8.01 (d, J = 1.8 Hz, 1H), 7.97 (d, J = 1.8 Hz, 1H), 7.82–7.70 (m, 7H), 7.61 (dd, J_1 = 7.9 Hz, J_2 = 1.8 Hz, 1H), 7.95–7.34 (m, 4H), 7.08–7.02 (m, 4H), 5.12 (q, J = 7.0 Hz, 1H), 4.61 (dd, J_1 = 13.0 Hz, J_2 =13.0 Hz, 2H), 4.16 (dd, J_1 = 13.0 Hz, J_2 = 13.0 Hz, 2H), 3.82 (s, 6H), 3.59–3.49 (m, 1H), 3.27–3.14 (m, 1H), 2.04–1.90 (m, 5H), 0.90 (t, J = 7.3 Hz); ^{13}C NMR (100 MHz, $CDCl_3$) δ 159.8$_2$, 159.8$_0$, 142.4, 142.1, 141.0$_5$, 140.9, 134.2, 133.2, 132.8, 131.5, 131.0, 130.2, 129.0, 128.5, 128.3, 128.2$_4$, 128.2$_1$, 127.1, 126.4, 126.3$_9$, 126.3$_4$, 126.3$_1$, 126.1, 114.8, 114.7, 71.7, 61.8, 60.8, 55.5, 17.3, 16.0, 10.8; FAB-MS (matrix: *m*-NBA) *m/z* 554 ([M-Br$^-$]$^+$ 50%); Anal. Calcd. for $C_{39}H_{40}BrNO_2 \cdot 0.35CHCl_3$: C, 69.87; H, 6.01; N, 2.07. Found: C, 69.94; H, 6.28; N, 2.28.

(*R*)-2,10-Bis(4-methoxyphenyl)-6-(1-phenylethyl)-6-propyl-6,7-dihydro-5*H*-dibenzo[*c,e*]azepin-6-ium bromide ((*R*)-2f)

Following general procedure was carried out with **1** (70.0 mg, 0.127 mmol), (*R*)-*N*-(1-phenylethyl)propan-1-amine [1] (23.1 mg, 0.142 mmol) and K_2CO_3 (110 mg, 0.799 mmol) in CH_3CN (4 mL) at 85 °C for 23 h. Purification using column chromatography ($CHCl_3$/MeOH, v/v 5:1) afforded ammonium salt (*R*)-**2f** (60.4 mg, 74% yield) as pale yellow solid: m.p. 124.3–125.0 °C; ^{1}H NMR (400 MHz, $CDCl_3$) δ 8.01 (d, J = 1.8 Hz, 1H), 7.97 (d, J = 1.8 Hz, 1H), 7.82–7.70 (m, 7H), 7.61 (dd, J_1 = 7.9 Hz, J_2 = 1.8 Hz, 1H), 7.95–7.34 (m, 4H), 7.08–7.02 (m, 4H), 5.12 (q, J = 7.0 Hz, 1H), 4.61 (dd, J_1 = 13.0 Hz, J_2 =13.0 Hz, 2H), 4.16 (dd, J_1 = 13.0 Hz, J_2 = 13.0 Hz, 2H), 3.82 (s, 6H), 3.59–3.49 (m, 1H), 3.27–3.14 (m, 1H), 2.04–1.90 (m, 5H), 0.90 (t, J = 7.3 Hz); ^{13}C NMR (100 MHz, $CDCl_3$) δ 159.8$_3$, 159.8$_0$, 142.4, 142.1, 141.0$_6$, 140.9, 134.2, 133.2, 132.8, 131.5, 131.0, 130.2, 129.0, 128.5, 128.3, 128.2$_4$, 128.2$_1$, 127.1, 126.4, 126.3$_5$, 126.3$_1$, 126.1, 114.8, 114.7,

71.7, 61.7, 60.8, 55.5, 17.3, 16.0, 10.8; FAB-MS (matrix: *m*-NBA) *m/z* 554 ([M-Br^-]$^+$ 40%); Anal. Calcd. for $C_{39}H_{40}BrNO_2 \cdot 0.35CHCl_3$: C, 69.87; H, 6.01; N, 2.07. Found: C, 69.65; H, 6.31; N, 2.13.

(*S*)-2,10-Bis(4-methoxyphenyl)-6-methyl-6-(1-phenylethyl)-6,7-dihydro-5*H*-dibenzo[*c*,*e*]azepin-6-ium bromide ((*S*)-2g)

Following general procedure was carried out with **1** (70.0 mg, 0.127 mmol), (*S*)-*N*-methyl-1-phenylethylamine (20.0 μL, 0.136 mmol) and K_2CO_3 (113.0 mg, 0.816 mmol) in CH_3CN (4 mL) at 65 °C for 23 h. Purification using column chromatography ($CHCl_3$/MeOH, v/v 20:1) afforded ammonium salt (*S*)-**2g** (56.5 mg, 74% yield) as pale yellow solid: m.p. 149.0–150.0 °C; ^{1}H NMR (400 MHz, $CDCl_3$) δ 8.08–8.07 (m, 2H), 7.83–7.69 (m, 10H), 7.55–7.51 (m, 3H), 7.09–7.04 (m, 4H), 4.92 (q, J = 6.8 Hz, 1H), 4.58 (d, J = 13.0 Hz, 1H), 4.14 (d, J = 13.0 Hz, 2H), 3.83 (s, 6H), 3.69 (d, J = 13.0 Hz, 1H), 3.12 (s, 3H),1.97, (d, J = 6.8Hz, 3H); ^{13}C NMR (100 MHz, $CDCl_3$) δ 159.9, 142.7$_3$, 142.7$_1$, 141.3$_4$, 141.3$_3$, 133.6, 132.8, 132.7, 131.6, 131.5, 131.0, 130.3, 129.1, 128.34, 128.32, 126.5, 126.4, 126.3, 126.2, 114.8, 71.3, 62.6, 61.2, 55.5, 44.3, 16.1; FAB-MS (matrix: *m*-NBA) *m/z* 526 ([M-Br^-]$^+$ 90%); Anal. Calcd. for $C_{37}H_{36}BrNO_2 \cdot 0.25CHCl_3$: C, 70.30; H, 5.74; N, 2.20. Found: C, 70.10; H, 6.04; N, 2.21.

(*R*)-2'-(Hydroxymethyl)-2,10-bis(4-methoxyphenyl)-5,7-dihydrospiro[dibenzo[*c*,*e*]azepine-6,1'-pyrrolidin]-6-ium bromide ((*R*)-2h)

Following general procedure was carried out with **1** (70.0 mg, 0.127 mmol), D-prolinol (13.0 μL, 0.134 mmol) and K_2CO_3 (112.0 mg, 0.810 mmol) in CH_3CN (4 mL) at 65 °C for 23 h. Purification using column chromatography ($CHCl_3$/MeOH, v/v 20:1) afforded ammonium salt (*R*)-**2h** (52.6 mg, 73% yield) as colorless solid: m.p. 302.1 °C (dec.); ^{1}H NMR (400 MHz, $CDCl_3$) δ 8.05–8.04 (m, 2H), 7.83–7.56 (m, 8H), 7.60 (dt, J_1 = 8.6 Hz, J_2 = 3.0, 4H), 5.18 (t, J = 4.6 Hz, 1H), 4.48 (dd, J_1 = 13.0 Hz, J_2 =13.0 Hz, 2H), 4.22–4.06 (m, 3H), 3.95–3.65 (m, 10H), 2.59–2.50 (m, 1H), 2.32–2.13 (m, 3H); ^{13}C NMR (100 MHz, $CDCl_3$) δ 159.8$_1$, 159.7$_9$, 142.7, 142.4, 141.2, 132.3, 132.1, 131.6$_4$, 131.6$_2$, 128.3$_2$, 128.2$_9$, 127.3, 127.0, 126.5, 126.4, 126.3, 114.8, 75.2, 63.4, 62.9, 59.3, 57.1, 55.5, 24.9, 19.8; FAB-MS (matrix: *m*-NBA) *m/z* 492 ([M-Br^-]$^+$ 100%); Anal. Calcd. for $C_{33}H_{34}BrNO_3 \cdot 0.18CH_2Cl_2$: C, 65.78; H, 5.76; N, 2.29. Found: C, 65.82; H, 5.59; N, 2.45.

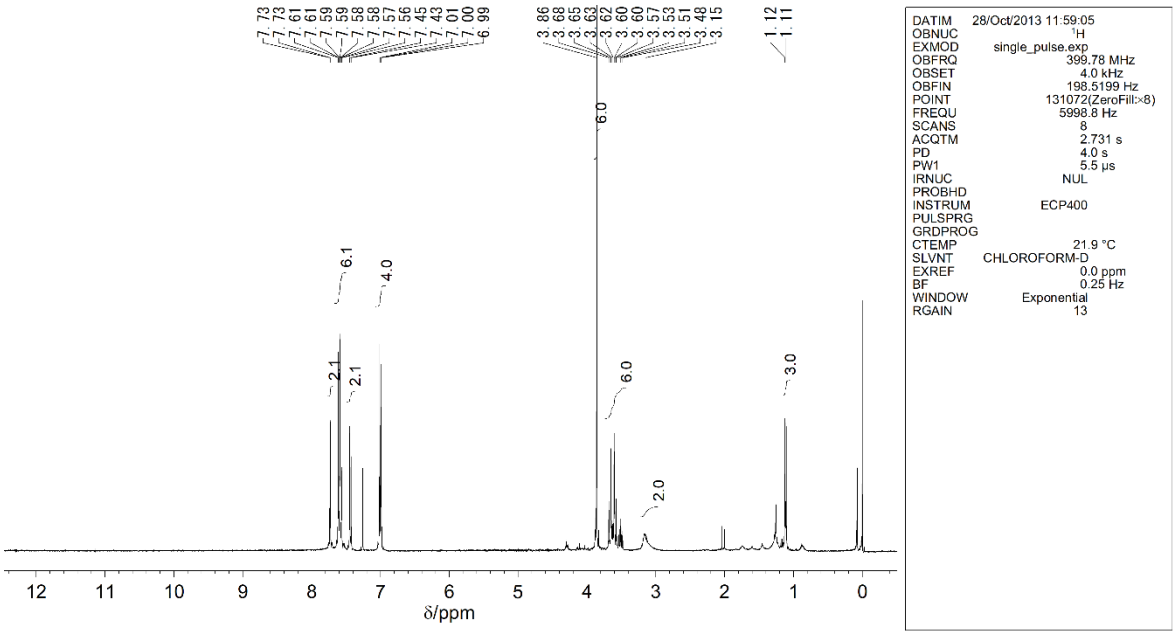

Figure S1. ^{1}H NMR Spectrum (400 MHz, $CDCl_3$) of (*S*)-**2a**

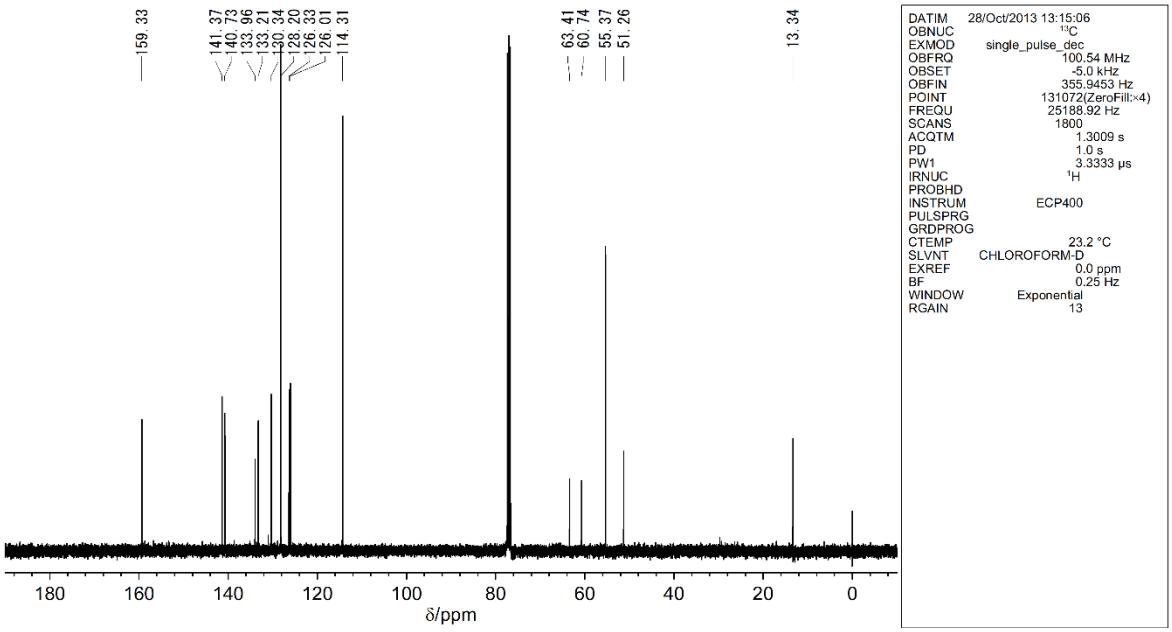

Figure S2. ^{13}C NMR Spectrum (100 MHz, $CDCl_3$) of (*S*)-**2a**

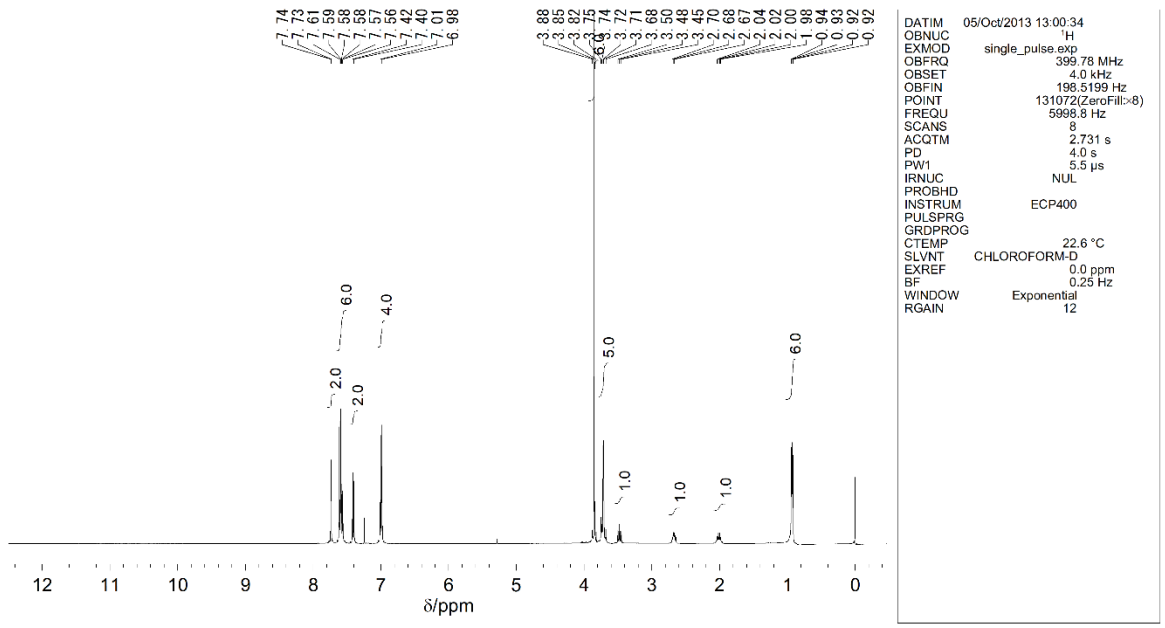

Figure S3. ^{1}H NMR Spectrum (400 MHz, $CDCl_3$) of (*S*)-**2b**

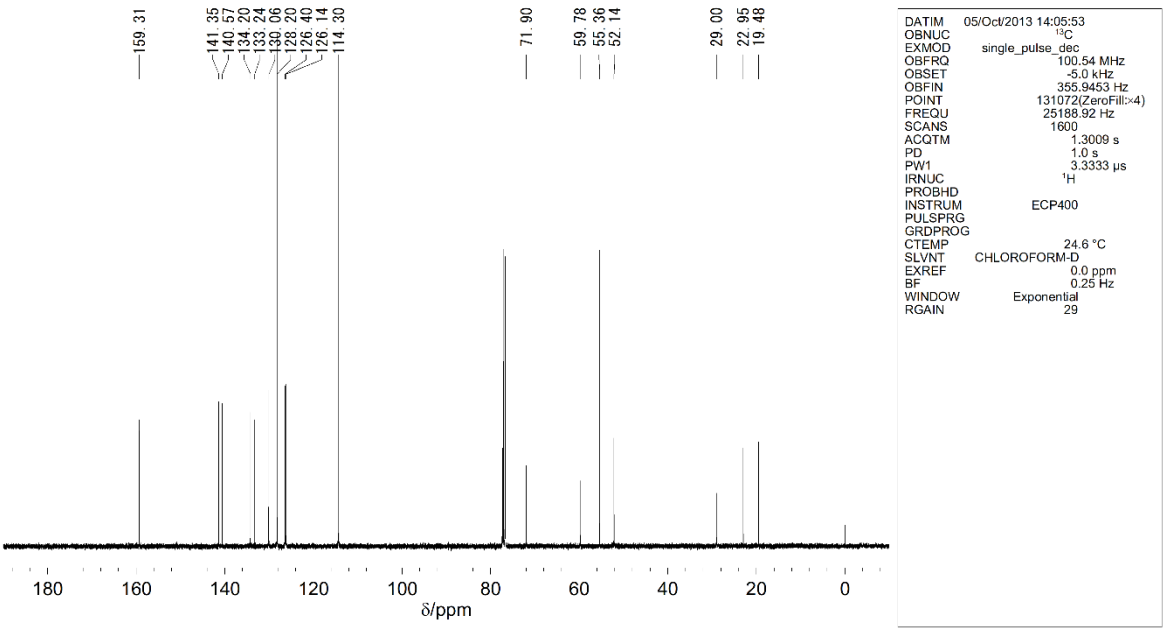

Figure S4. ^{13}C NMR Spectrum (100 MHz, $CDCl_3$) of (*S*)-**2b**

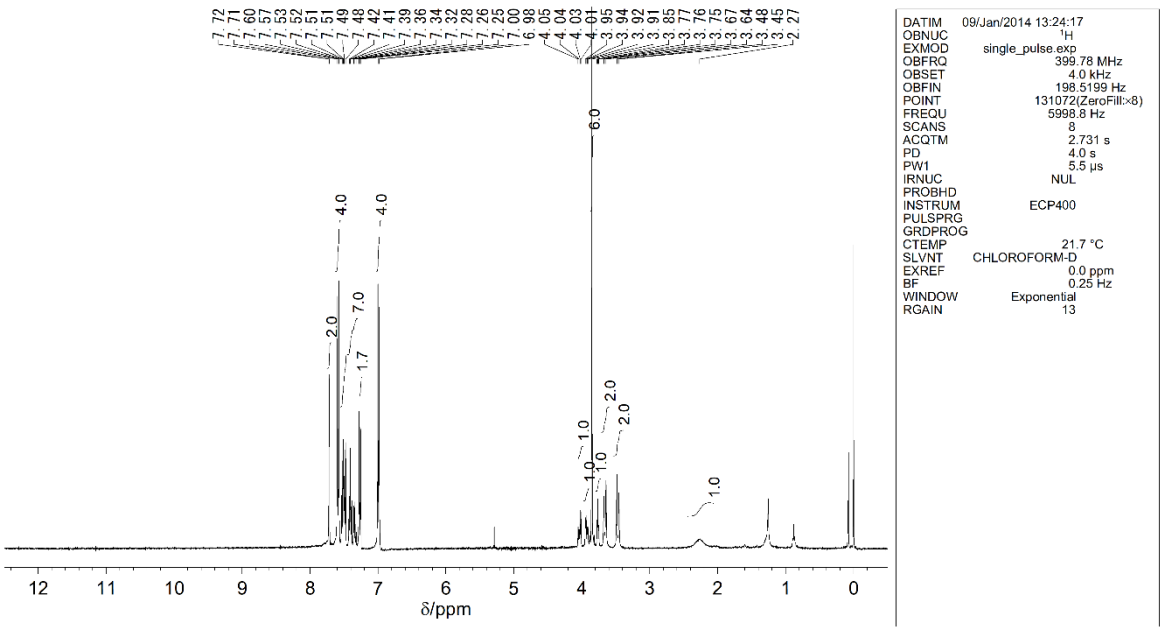

Figure S5. ^{1}H NMR Spectrum (400 MHz, $CDCl_3$) of (*S*)-**2c**

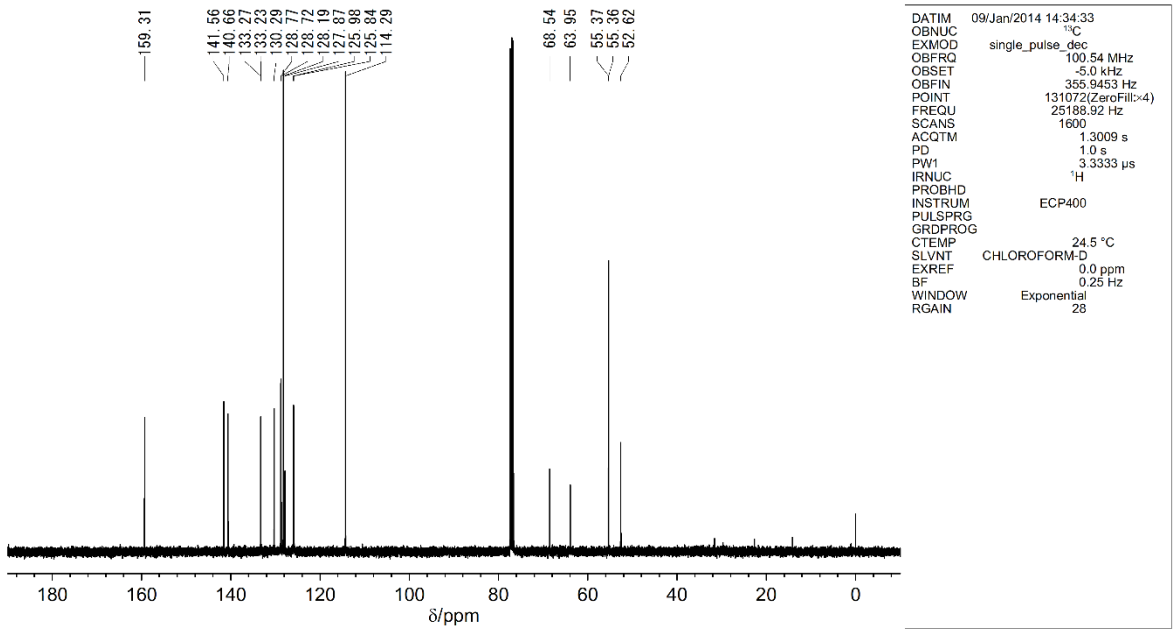

Figure S6. ^{13}C NMR Spectrum (100 MHz, $CDCl_3$) of (*S*)-**2c**

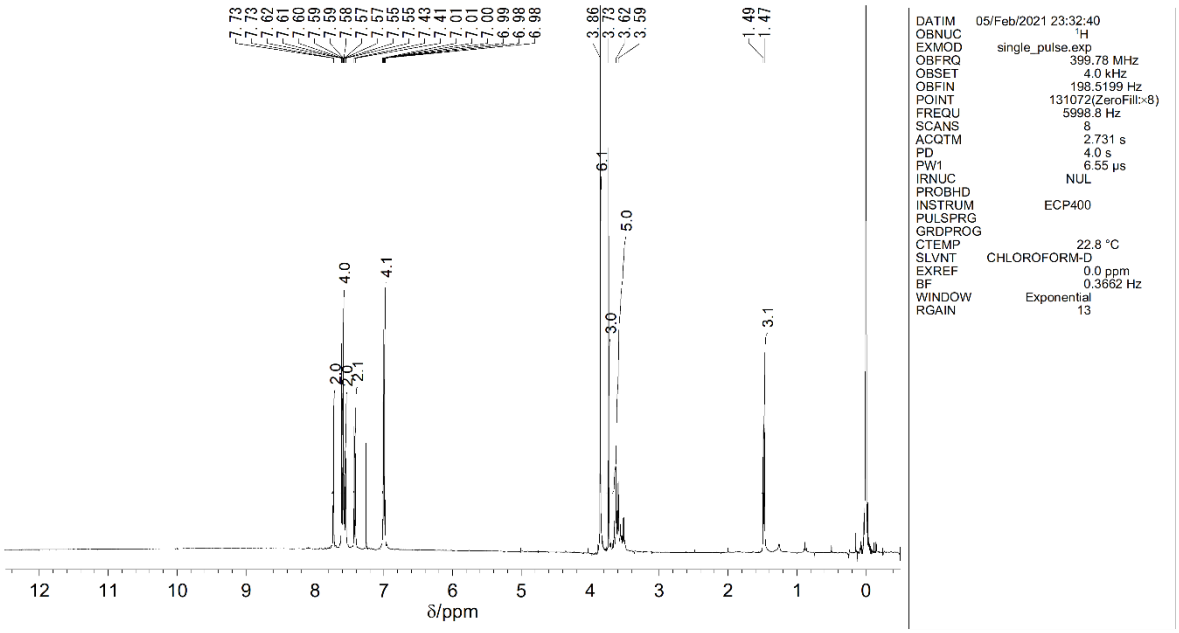

Figure S7. ^{1}H NMR Spectrum (400 MHz, $CDCl_3$) of (*S*)-**2d**

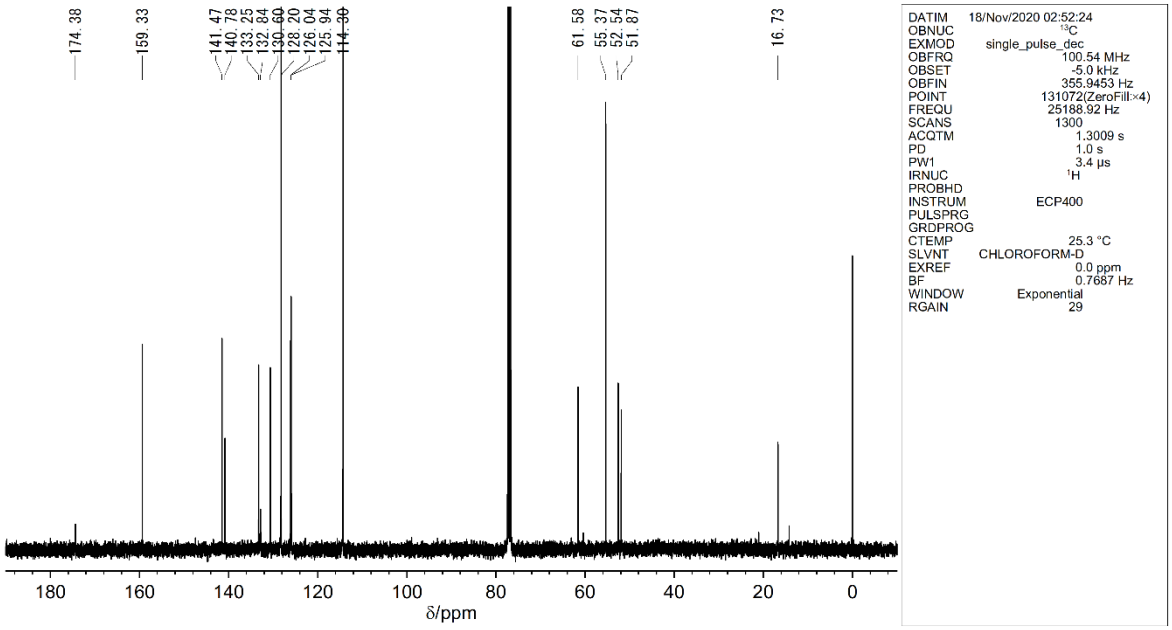

Figure S8. ^{13}C NMR Spectrum (100 MHz, $CDCl_3$) of (*S*)-**2d**

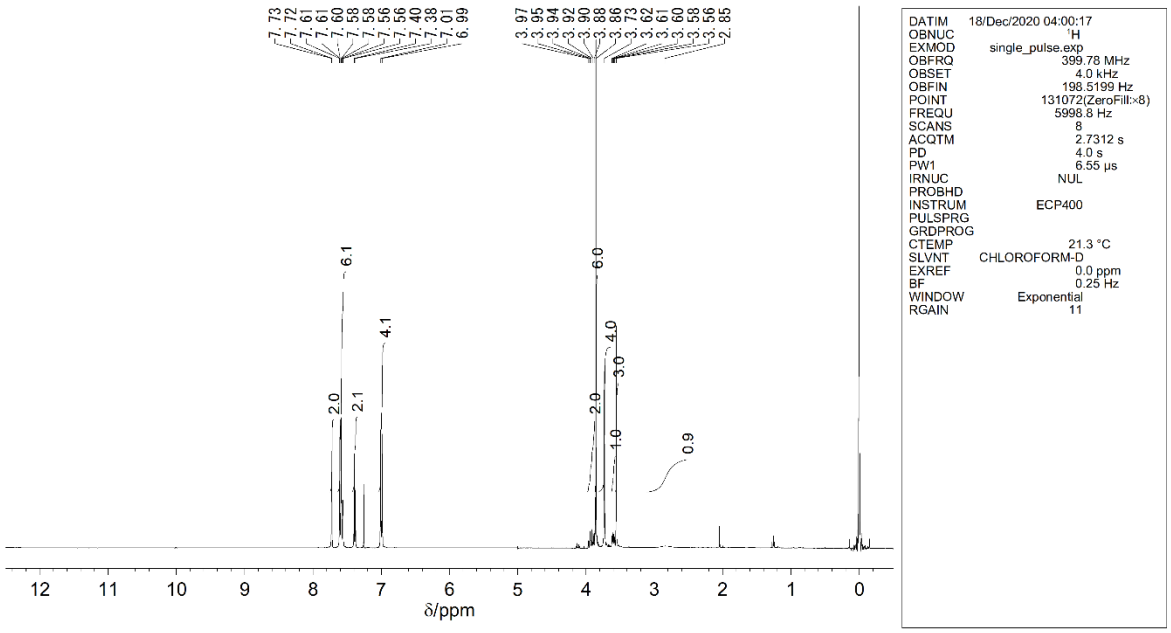

Figure S9. ^{1}H NMR Spectrum (400 MHz, $CDCl_3$) of (*S*)-**2e**

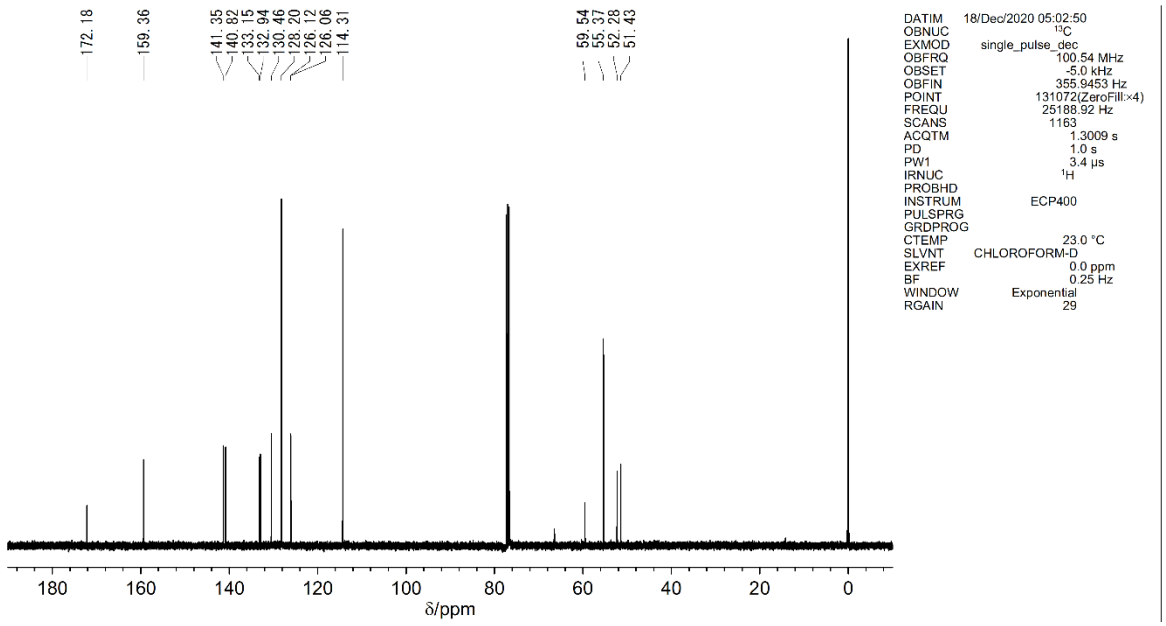

Figure S10. ^{13}C NMR Spectrum (100 MHz, $CDCl_3$) of (*S*)-**2e**

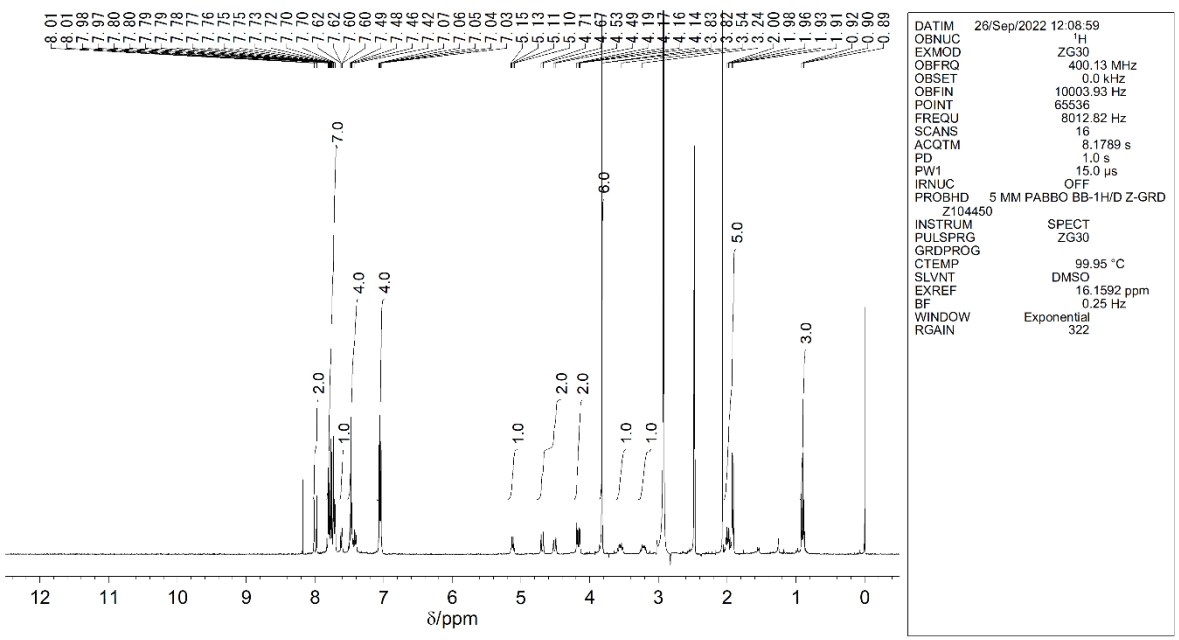

Figure S11. ^{1}H NMR Spectrum (400 MHz, DMSO-d_6, 373K) of (*S*)-**2f**

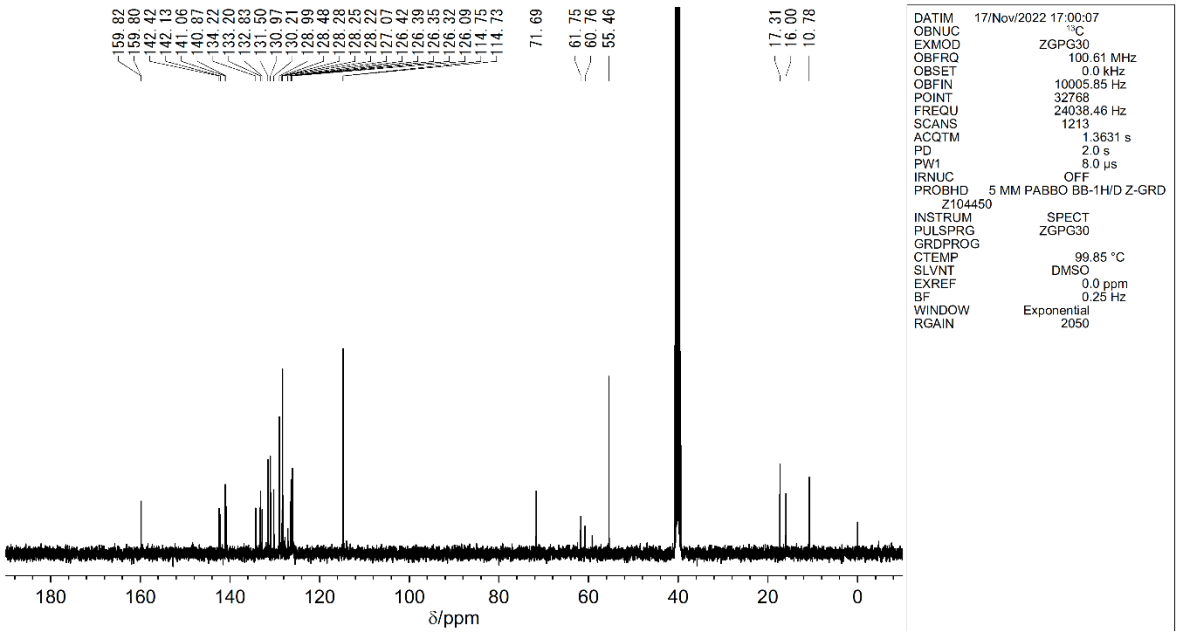

Figure S12. ^{13}C NMR Spectrum (100 MHz, DMSO-d_6, 373K) of (*S*)-**2f**

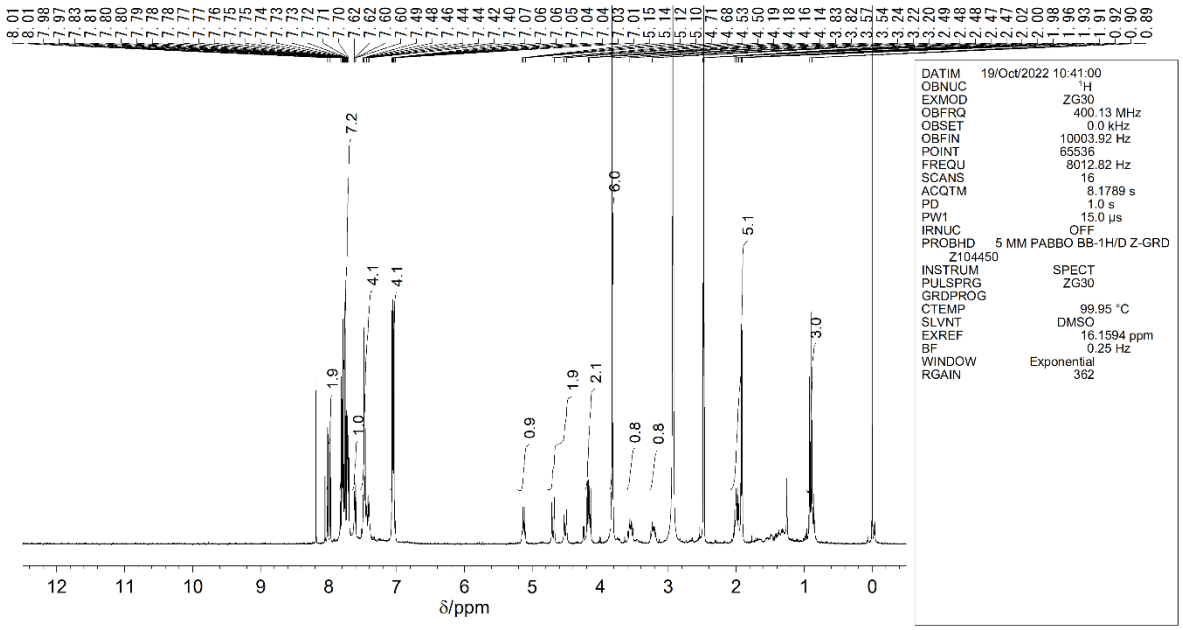

Figure S13. [1]H NMR Spectrum (400 MHz, DMSO-d_6, 373K) of (*R*)-**2f**

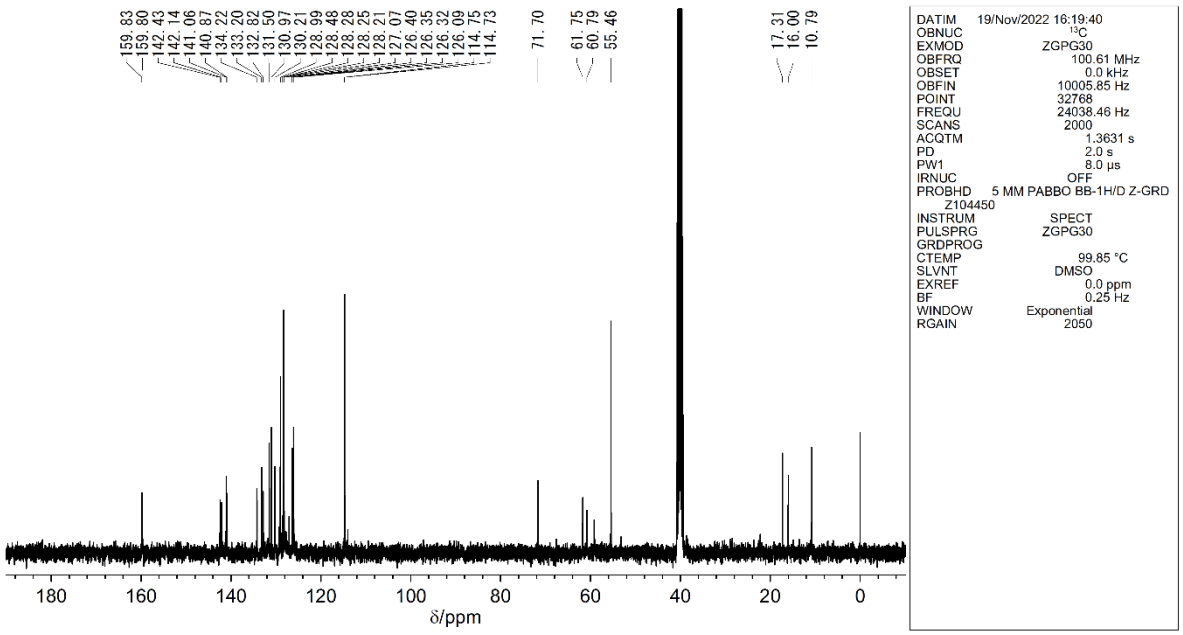

Figure S14. [13]C NMR Spectrum (100 MHz, DMSO-d_6, 373K) of (*R*)-**2f**

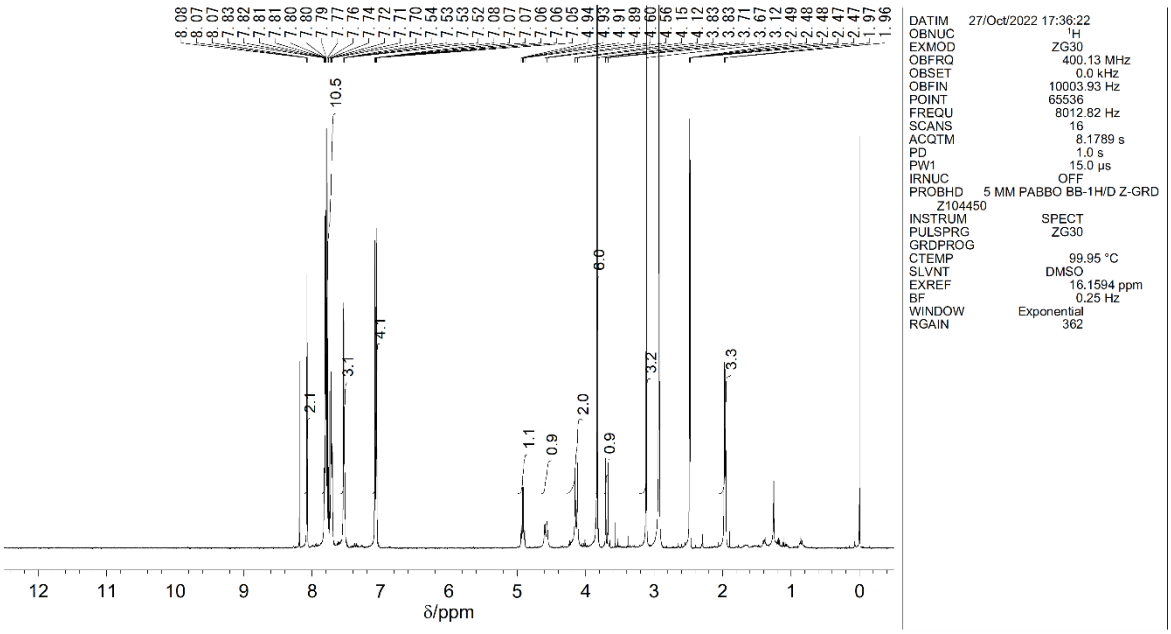

Figure S15. ^{1}H NMR Spectrum (400 MHz, DMSO-d_6, 373K) of (*S*)-**2g**

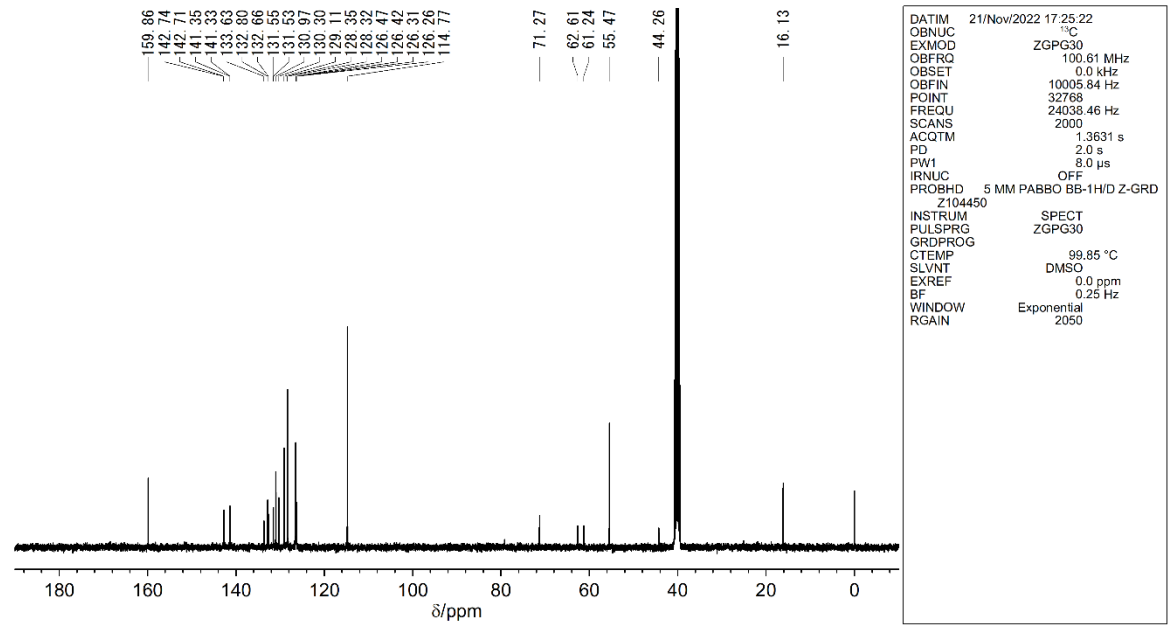

Figure S16. ^{13}C NMR Spectrum (100 MHz, DMSO-d_6, 373K) of (*S*)-**2g**

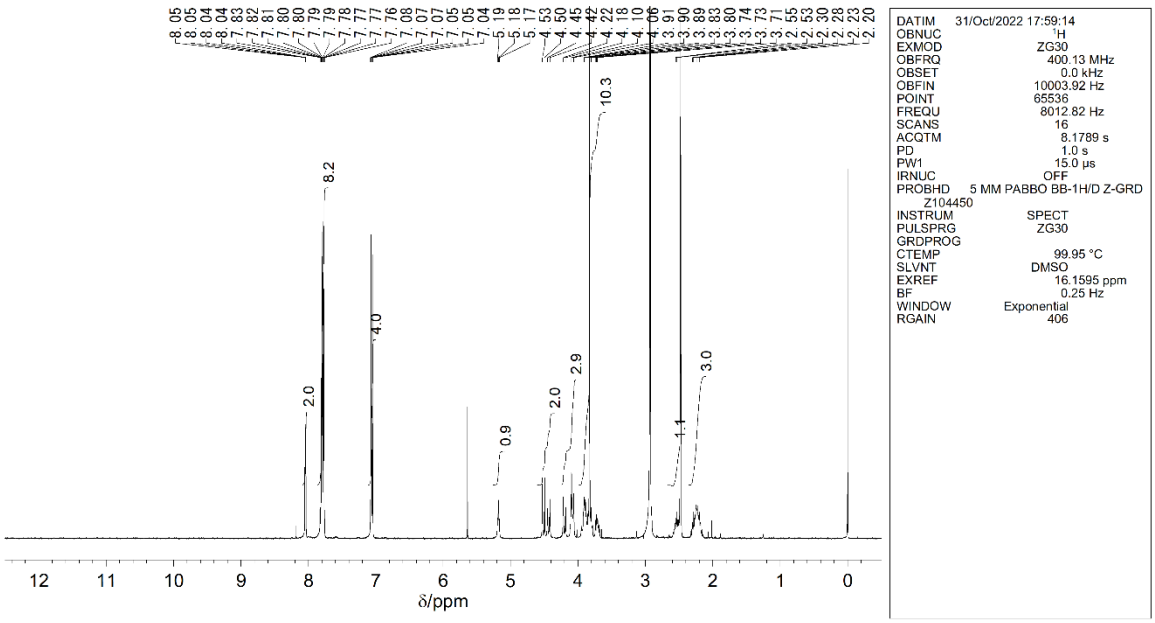

Figure S17. [1]H NMR Spectrum (400 MHz, DMSO-d_6, 373K) of (*R*)-**2h**

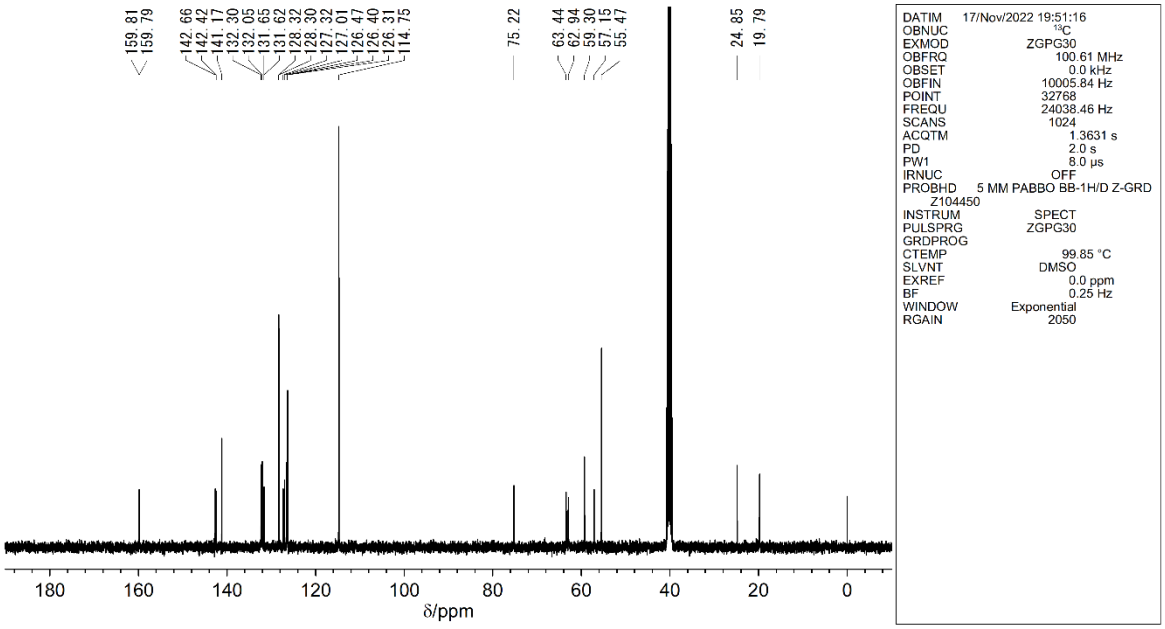

Figure S18. [13]C NMR Spectrum (100 MHz, DMSO-d_6, 373K) of (*R*)-**2h**

Table S1. CD spectral data of (*S*)-**2a**–**e**,**i**–**n**[a]

Entry	Predicted helicity		$\Delta\varepsilon_1$[b] (λ [nm])	$\Delta\varepsilon_2$[b] (λ [nm])	Experimental helicity	CD amplitude (A_{CD} value)[c]
1	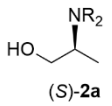 (*S*)-**2a**	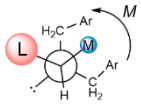	–0.6 (277.6)	+1.7 (257.6)	*M*	–2.3
2	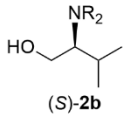 (*S*)-**2b**	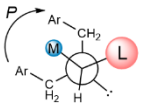	+3.1 (280.0)	–0.9 (255.6)	*P*	+4.0
3	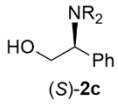 (*S*)-**2c**	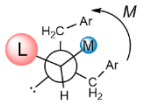	–8.6 (287.2)	+10.6 (261.2)	*M*	–19.2
4	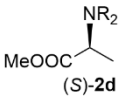 (*S*)-**2d**	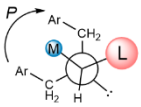	+5.9 (285.6)	–4.4 (261.1)	*P*	+10.3
5	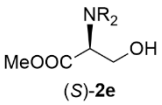 (*S*)-**2e**	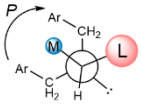	+8.2 (283.6)	–5.8 (257.8)	*P*	+14.0
6[c]	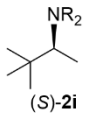 (*S*)-**2i**	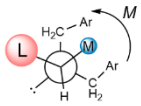	–9.2 (278.8)	+8.5 (256.2)	*M*	–17.7
7[c]	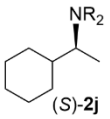 (*S*)-**2j**	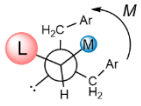	–3.5 (279.4)	+4.0 (257.2)	*M*	–7.5
8[c]	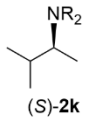 (*S*)-**2k**	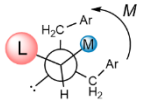	–2.4 (281.4)	+3.5 (255.0)	*M*	–5.9
9[c]	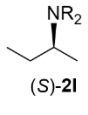 (*S*)-**2l**	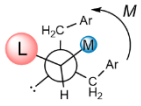	–0.6 (282.6)	+1.2 (260.2)	*M*	–1.8
10[c]	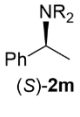 (*S*)-**2m**	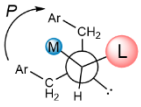	+9.8 (286.8)	–10.6 (261.2)	*P*	+20.4
11[c]	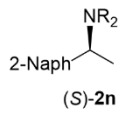 (*S*)-**2n**	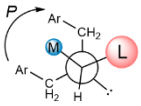	+7.2 (287.4)	–15.0 (258.4)	*P*	+22.2

[a] All CD data were measured in CH_3CN, 2 x 10^{-4} M concentration using 1 mm CD cell at 293 K. [b] $\Delta\varepsilon_1$ and $\Delta\varepsilon_2$ are intensities of first and second Cotton effects. [c] A_{CD} value: $A_{CD} = \Delta\varepsilon_1 - \Delta\varepsilon_2$, where $\Delta\varepsilon_1$ and $\Delta\varepsilon_2$ are intensities of first and second Cotton effects, respectively. [c] Kuwahara, S.; Nakamura, M.; Yamaguchi, A.; Ikeda, M.; Habata, Y. *Org. Lett.* **2013**, 15, 5738–5741.

Table S2. CD spectral data of (*S*)-**2f**–**h**[a].

Entry	Compound	$\Delta\varepsilon_1$[b] (λ [nm])	$\Delta\varepsilon_2$[b] (λ [nm])	Experimental helicity	CD amplitude (A_{CD} value)[c]
1	(*S*)-**2f**	–7.0 (292.6)	+5.5 (266.0)	*M*	–12.5
2	(*S*)-**2g**	–15.3 (292.3)	+6.3 (265.1)	*M*	–21.6
3	(*S*)-**2h**	+19.3 (291.1)	–13.5 (265.6)	*P*	+32.8

[a] All CD data were measured in CH_3CN, 2 x 10^{-4} M concentration using 1 mm CD cell at 293 K. [b] $\Delta\varepsilon_1$ and $\Delta\varepsilon_2$ are intensities of first and second Cotton effects. [c] A_{CD} value: $A_{CD} = \Delta\varepsilon_1 - \Delta\varepsilon_2$, where $\Delta\varepsilon_1$ and $\Delta\varepsilon_2$ are intensities of first and second Cotton effects, respectively.

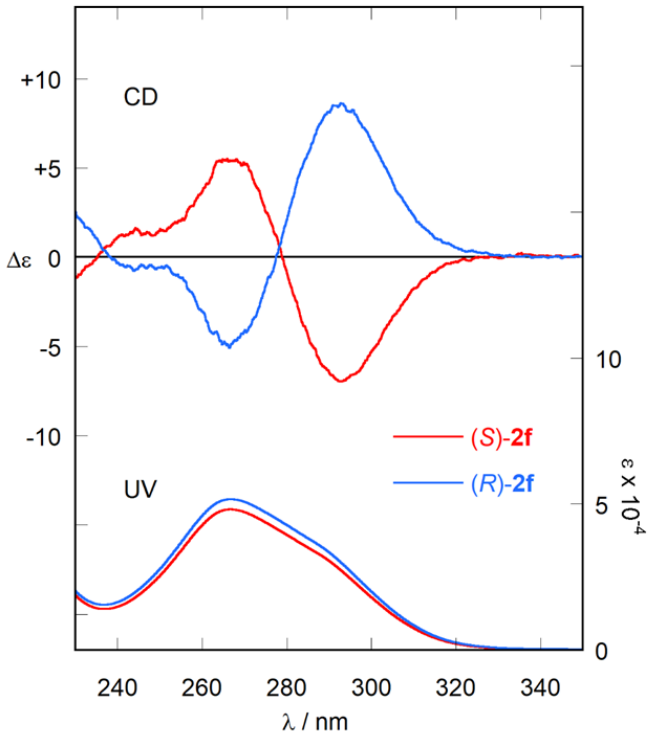

Figure S19. CD and UV spectra of (*S*)-**2f** and (*R*)-**2f** (2×10^{-4} M in CH_3CN, 293 K).

Theoretical calculations at B3LYP/6-31G* level

Table S3. Calculated conformers of (*S*)-**3a** at B3LYP/6-31G* level.

Entry	Conformer	Helicity	Dihedral angle[a]	*E*, kJ/mol	*K*[b]	Population, %
1	#M1	*M*	−42.64	0.00	1.00	47.9
2	#P1	*P*	43.25	0.25	0.90	43.2
3	#P3	*P*	43.01	5.52	0.10	5.0
4	#M3	*M*	−42.75	6.14	0.08	3.9

[a] Dihedral angle of C6-C1-C1'-C6'. [b] Equilibrium constant at 298 K.

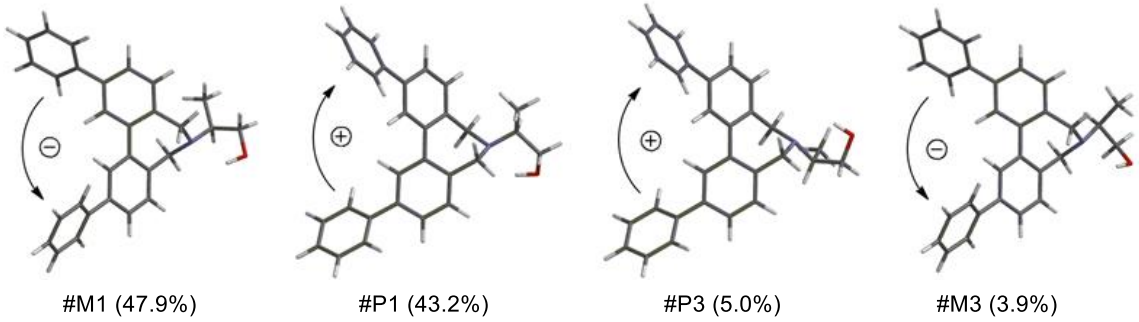

Figure S20. Four major conformers of (*S*)-**3a** at B3LYP/6-31G* level.

Table S4. Calculated conformers of (*S*)-**3b** at B3LYP/6-31G* level.

Entry	Conformer	Helicity	Dihedral angle[a]	*E*, kJ/mol	*K*[b]	Population, %
1	#M1	*M*	−41.67	0.00	1.00	23.1
2	#P4	*P*	42.51	1.05	0.65	15.0
3	#P6	*P*	42.71	2.76	0.32	7.4
4	#P92	*P*	43.56	3.09	0.28	6.5
5	#P73	*P*	43.17	3.18	0.27	6.3
6	#M3	*M*	−43.71	3.30	0.26	6.0
7	#P1	*P*	41.34	3.43	0.24	5.7
8	#P39	*P*	42.54	3.43	0.24	5.7
9	#P2	*P*	42.94	3.51	0.24	5.5
10	#M5	*M*	−41.63	4.01	0.19	4.4
11	#P12	*P*	42.19	4.56	0.15	3.6
12	#P22	*P*	42.17	5.69	0.10	2.2
13	#P25	*P*	42.45	5.69	0.10	2.2
14	#M13	*M*	−42.23	6.23	0.08	1.8
15	#M26	*M*	−43.51	6.40	0.07	1.7
16	#P99	*P*	43.45	7.61	0.04	1.0
17	#P8	*P*	43.17	8.45	0.03	0.7
18	#M9	*M*	−43.15	9.87	0.02	0.4

[a] Dihedral angle of C6-C1-C1'-C6'. [b] Equilibrium constant at 298 K.

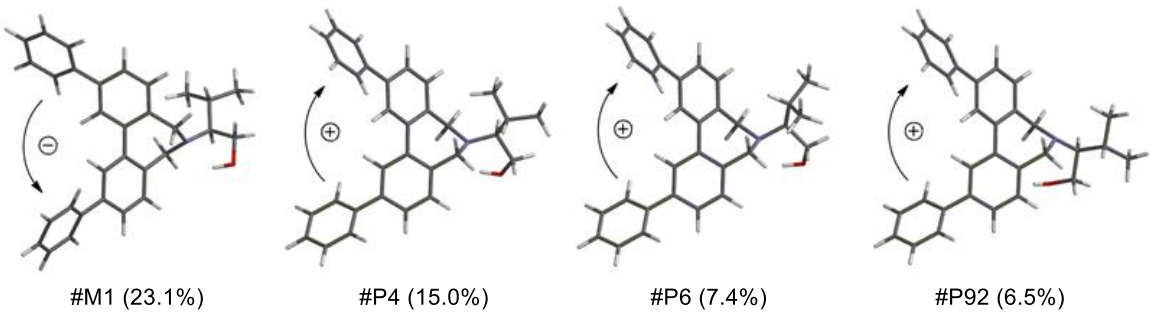

Figure S21. Four major conformers of (*S*)-**3b** at B3LYP/6-31G* level.

Table S5. Calculated conformers of (*S*)-**3c** at B3LYP/6-31G* level.

Entry	Conformer	Helicity	Dihedral angle[a]	*E*, kJ/mol	*K*[b]	Population, %
1	#M3	*M*	−45.52	0.00	1.00	48.7
2	#P1	*P*	43.01	2.64	0.34	16.5
3	#M6	*M*	−42.96	3.80	0.21	10.2
4	#P6	*P*	42.01	4.69	0.15	7.1
5	#M10	*M*	−42.39	5.63	0.10	4.8
6	#M16	*M*	−42.06	5.72	0.10	4.7
7	#M7	*M*	−41.95	5.81	0.09	4.5
8	#P20	*P*	43.33	7.50	0.05	2.2
9	#P13	*P*	42.97	8.83	0.03	1.3

[a] Dihedral angle of C6-C1-C1'-C6'. [b] Equilibrium constant at 298 K.

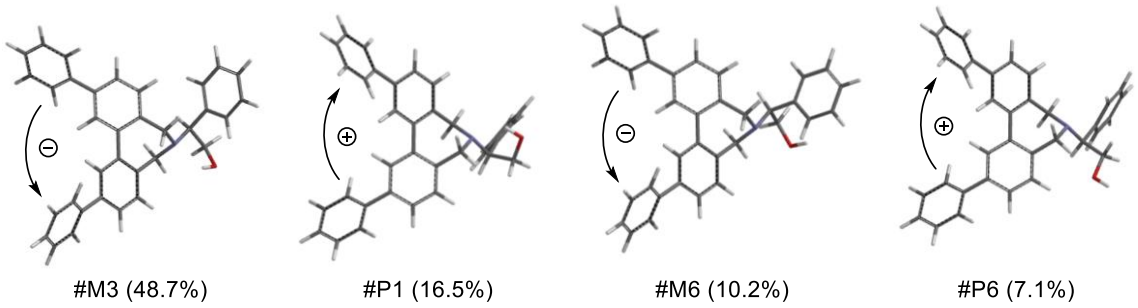

Figure S22. Three major conformers of (*S*)-**3c** at B3LYP/6-31G* level.

Table S6. Calculated conformers of (*S*)-**3d** at B3LYP/6-31G* level.

Entry	Conformer	Helicity	Dihedral angle[a]	*E*, kJ/mol	*K*[b]	Population, %
1	#P1	*P*	42.31	0.00	1.00	63.2
2	#M1	*M*	−42.62	3.15	0.27	17.4
3	#M3	*M*	−42.65	4.69	0.15	9.2
4	#P5	*P*	42.02	5.93	0.09	5.5
5	#M9	*M*	−42.61	8.18	0.03	2.2
6	#P3	*P*	43.06	9.38	0.02	1.3
7	#P9	*P*	43.82	9.92	0.02	1.1

[a] Dihedral angle of C6-C1-C1'-C6'. [b] Equilibrium constant at 298 K.

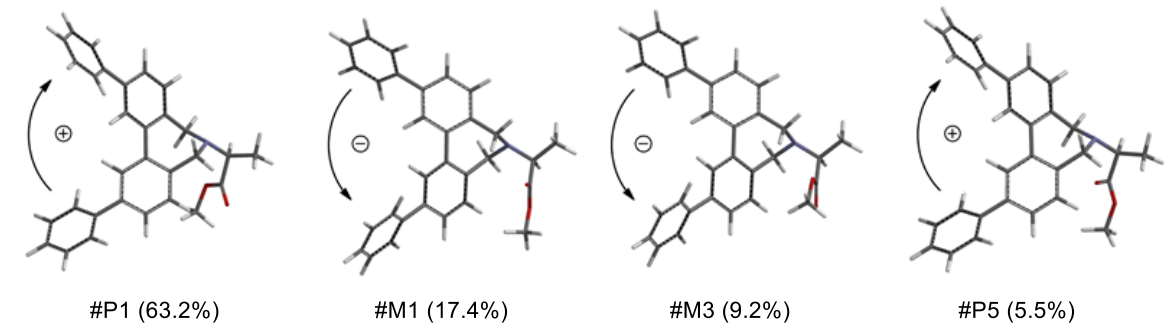

Figure S23. Four major conformers of (*S*)-**3d** at B3LYP/6-31G* level.

Table S7. Calculated conformers of (*S*)-**3e** at B3LYP/6-31G* level.

Entry	Conformer	Helicity	Dihedral angle[a]	*E*, kJ/mol	*K*[b]	Population, %
1	#P12	*P*	42.77	0	1.00	34.7
2	#P2	*P*	42.08	0.27	0.90	31.0
3	#P14	*P*	41.69	2.48	0.36	12.5
4	#M19	*M*	−43.55	4.15	0.18	6.3
5	#M1	*M*	−43.05	4.32	0.17	5.9
6	#M20	*M*	−42.27	4.59	0.15	5.3
7	#M3	*M*	−43.51	7.63	0.04	1.5
8	#P4	*P*	42.00	8.12	0.04	1.2
9	#M56	*M*	−43.15	8.76	0.03	1.0
10	#M15	*M*	−42.54	9.71	0.02	0.6

[a] Dihedral angle of C6-C1-C1'-C6'. [b] Equilibrium constant at 298 K.

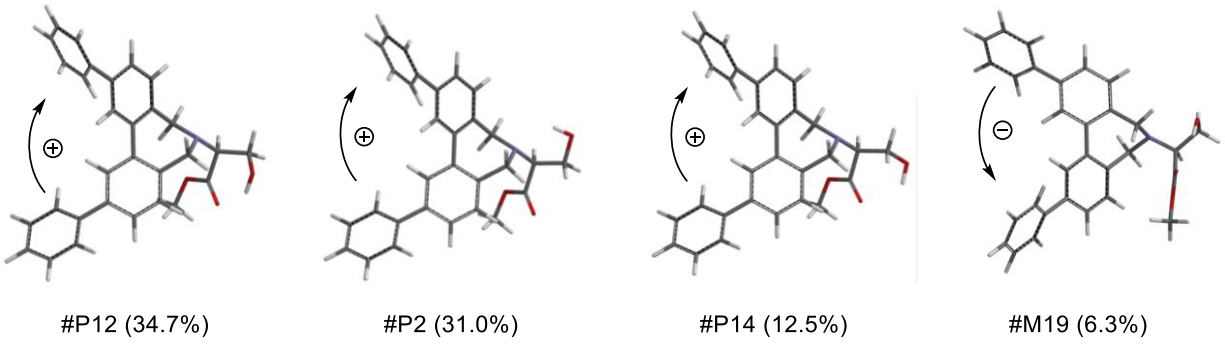

Figure S24. Four major conformers of (*S*)-**3e** at B3LYP/6-31G* level.

Table S8. Calculated conformers of (*S*)-**3f** at B3LYP/6-31G* level.

Entry	Conformer	Helicity	Dihedral angle[a]	*E*, kJ/mol	*K*[b]	Population, %
1	#M3	*M*	−41.74	0.00	1.00	53.5
2	#P1	*P*	40.44	2.95	0.30	15.9
3	#M2	*M*	−41.81	3.57	0.23	12.4
4	#P4	*P*	42.39	5.02	0.13	6.8
5	#P5	*P*	42.08	5.95	0.09	4.7
6	#M6	*M*	−43.02	7.42	0.05	2.5
7	#M1	*M*	−40.24	8.54	0.03	1.6
8	#P2	*P*	39.83	8.95	0.03	1.4
9	#M5	*M*	−40.90	9.18	0.02	1.2

[a] Dihedral angle of C6-C1-C1'-C6'. [b] Equilibrium constant at 298 K.

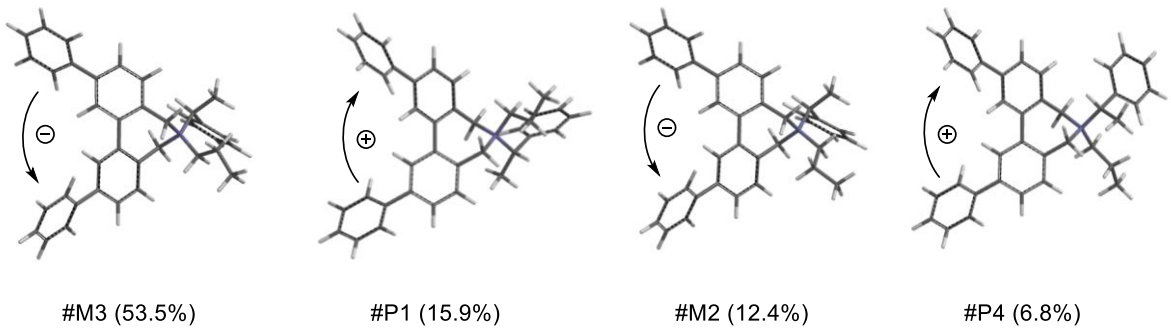

Figure S25. Four major conformers of (*S*)-**3f** at B3LYP/6-31G* level.

Table S9. Calculated conformers of (*S*)-**3g** at B3LYP/6-31G* level.

Entry	Conformer	Helicity	Dihedral angle[a]	*E*, kJ/mol	*K*[b]	Population, %
1	#M2	*M*	−43.39	0.00	1.00	73.5
2	#P1	*P*	42.25	2.49	0.36	26.5

[a] Dihedral angle of C6-C1-C1'-C6'. [b] Equilibrium constant at 298 K.

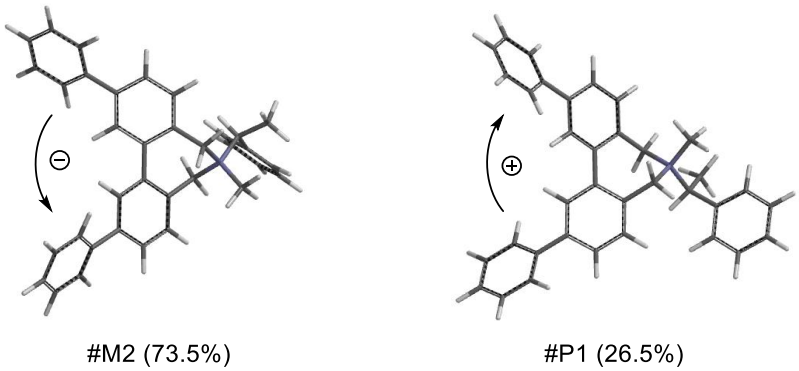

Figure S26. Two major conformers of (*S*)-**3g** at B3LYP/6-31G* level.

Table S10. Calculated conformers of (*R*)-**3h** at B3LYP/6-31G* level.

Entry	Conformer	Helicity	Dihedral angle[a]	*E*, kJ/mol	*K*[b]	Population, %
1	#P3	*P*	42.49	0.00	1.00	57.3
2	#M4	*M*	−42.59	4.63	0.15	8.6
3	#M7	*M*	−41.95	5.10	0.12	7.1
4	#P1	*P*	42.55	5.57	0.10	5.8
5	#P2	*P*	43.32	5.93	0.09	5.0
6	#P11	*P*	43.92	6.27	0.08	4.4
7	#P6	*P*	43.76	6.69	0.06	3.7
8	#P22	*P*	43.92	6.83	0.06	3.5
9	#P5	*P*	43.10	7.99	0.04	2.2
10	#P8	*P*	39.96	8.71	0.03	1.6
11	#P9	*P*	40.57	9.90	0.02	1.0

[a] Dihedral angle of C6-C1-C1'-C6'. [b] Equilibrium constant at 298 K.

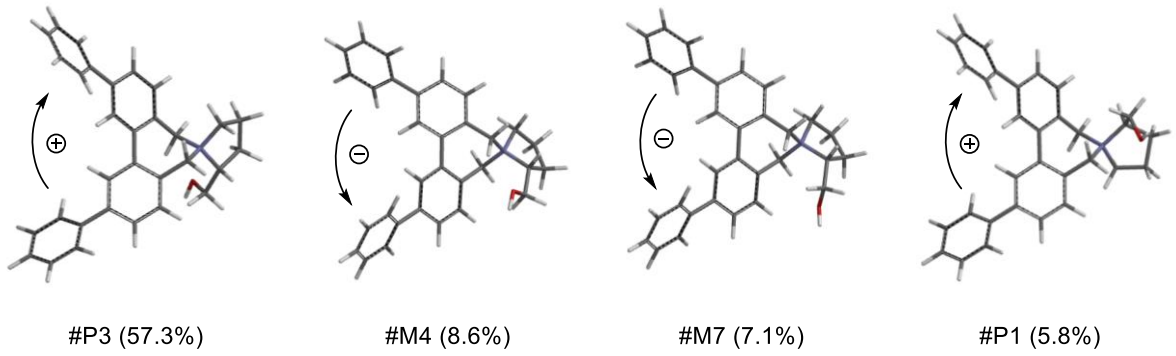

Figure S27. Four major conformers of (*R*)-**3h** at B3LYP/6-31G* level.

Table S11. Comparison of the excess of *P* conformer and observed CD amplitude at B3LYP/6-31G* level.

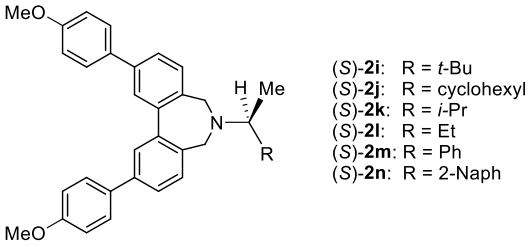

Entry	Compound	Calcurated ratio (*P/M*)	Excess of *P* confomer, %[a]	Observed CD amplitude (A_{CD} value)[b]
1	(*S*)-**2a**	48.2:51.8	–3.6	–2.3
2	(*S*)-**2b**	62.3:37.7	24.6	+4.0
3	(*S*)-**2c**	27.1:72.9	–45.8	–19.2
4	(*S*)-**2d**	71.2:28.8	42.4	+10.3
5	(*S*)-**2e**	79.4:20.6	58.8	+14.0
6	(*S*)-**2f**	28.8:71.2	–42.4	–12.5
7	(*S*)-**2g**	26.5:73.5	–47.0	–21.6
8	(*R*)-**2h**	84.4:15.6	68.8	+32.8
9[c]	(*S*)-**2i**	24.8:75.2	–50.4	–17.7
10[c]	(*S*)-**2j**	44.0:56.0	–12.0	–7.5
11[c]	(*S*)-**2k**	42.4:57.6	–15.2	–5.9
12[c]	(*S*)-**2l**	47.2:52.8	–5.6	–1.8
13[c]	(*S*)-**2m**	69.0:31.0	38.0	+20.4
14[c]	(*S*)-**2n**	77.3:22.7	54.6	+22.2

[a] Excess of *P* conformer (%) = ([*P*]–[*M*])/([*P*]+[*M*])×100, where [*P*] and [*M*] are the amounts of *P* and *M* conformers calculated by B3LYP/6-31G*. [b] A_{CD} value: $A_{CD} = \Delta\varepsilon_1 - \Delta\varepsilon_2$, where $\Delta\varepsilon_1$ and $\Delta\varepsilon_2$ are intensities of first and second Cotton effects, respectively. [c] Kuwahara, S.; Nakamura, M.; Yamaguchi, A.; Ikeda, M.; Habata, Y. *Org. Lett.* **2013**, 15, 5738–5741.

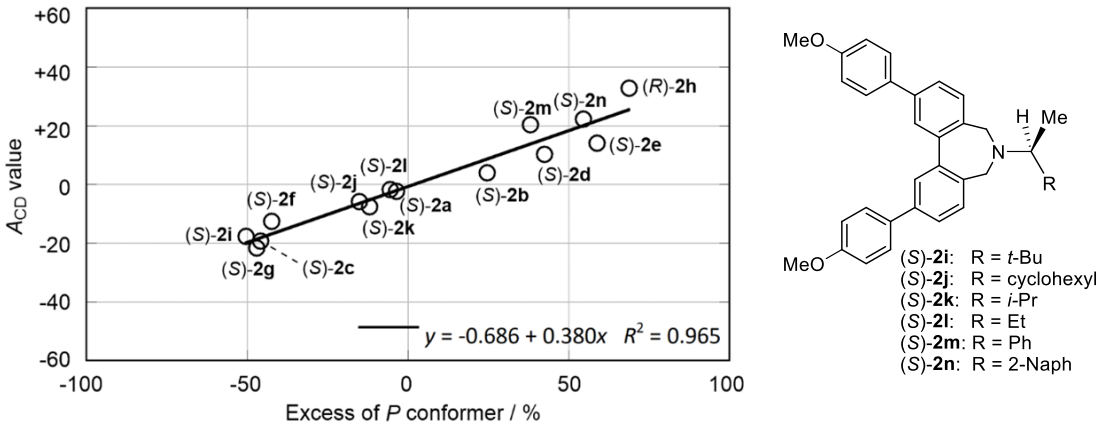

Figure S28. The relationship between the A_{CD} values and excess of *P* conformer. Excess of *P* conformer (%) = ([*P*]–[*M*])/([*P*]+[*M*])×100, where [*M*] and [*P*] are the amounts of *P* and *M* conformers calculated by B3LYP/6-31G*, respectively.

X-ray structure determination

Crystals of (*S*)-**2b** was mounted on the top of a glass fiber, and the data collection was carried out on a Bruker SMART diffractometer equipped with a CCD area detector at 120 K. The data were corrected for Lorentz and polarization effects, and absorption corrections were applied with the *SADABS* probram [3]. The structure was solved by direct methods and subsequent difference Fourier syntheses using the program *SHELXTL* [4]. All non-H atoms were refined anisotropically, and H atoms were placed in calculated positions and thereafter refined with U_{iso}(H) = 1.2U_{eq}(C).

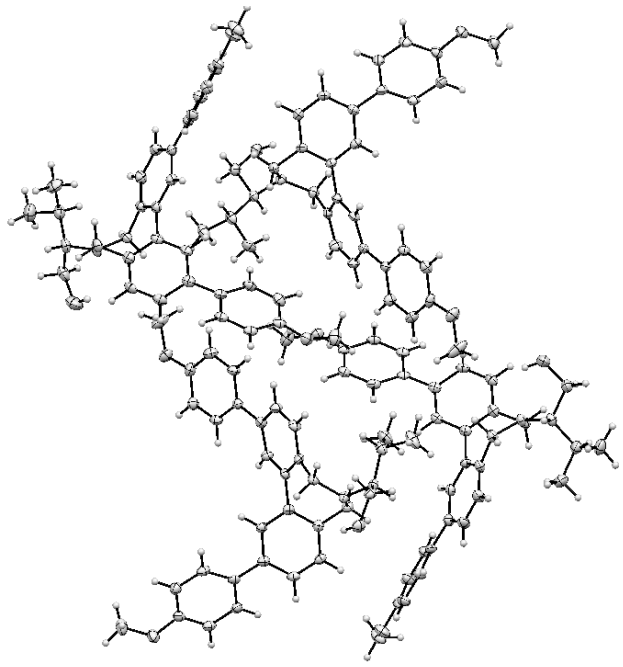

Figure S29. ORTEP The drawing of (*S*)-**2b**.

Table S12. Crystal data and structure refinement for (*S*)-**2b**

Identification code	tri_p1	
Empirical formula	C33 H35 N O3	
Formula weight	493.62	
Temperature	120 K	
Wavelength	0.71073 Å	
Crystal system	Triclinic	
Space group	P1	
Unit cell dimensions	a = 9.5731(4) Å	α = 99.0630(10)°.
	b = 15.1084(7) Å	β = 94.8370(10)°.
	c = 19.7050(9) Å	γ = 108.2140(10)°.
Volume	2646.2(2) Å^3	
Z	4	
Density (calculated)	1.239 Mg/m^3	
Absorption coefficient	0.078 mm^{-1}	
F(000)	1056	
Crystal size	0.32 x 0.26 x 0.12 mm^3	
Theta range for data collection	1.06 to 27.48°.	
Index ranges	-12 <= h <= 12, -19 <= k <= 14, -22 <= l <= 25	
Reflections collected	17127	
Independent reflections	14002 [R(int) = 0.0217]	
Completeness to theta = 27.48°	98.9 %	
Absorption correction	Empirical	
Max. and min. transmission	0.9906 and 0.9754	
Refinement method	Full-matrix least-squares on F^2	
Data / restraints / parameters	14002 / 3 / 1353	
Goodness-of-fit on F^2	1.022	
Final R indices [I > 2sigma(I)]	R_1 = 0.0459, wR_2 = 0.0981	
R indices (all data)	R_1 = 0.0614, wR_2 = 0.1090	
Absolute structure parameter	0.4(9)	
Largest diff. peak and hole	0.229 and -0.255 e.Å^{-3}	

References

[1] Kuwahara, S.; Chamura, R.; Tsuchiya, S.; Ikeda, M.; Habata,Y. *Chem. Commun.* **2013**, *49*, 2186–2188.

[2] Spartan'18, Irvine, CA; Wavefunction, 2018.

[3] Sheldrick, G. M. *Program for absorption correction of area detector frames*; Madison, WI; Bruker AXS, Inc., 1996.

[4] *SHELXTL*, *version 5.1*; Madison, WI; Bruker AXS, Inc., 1997.